

# On the short time dynamics of dense polymeric systems and the origin of the glass transition: A model system

Andrzej Kolinski,<sup>a)</sup> Jeffrey Skolnick,<sup>b)</sup> and Robert Yaris

*Department of Chemistry, Washington University, St. Louis, Missouri 63130*

(Received 23 August 1985; accepted 1 November 1985)

In order to model the short time (and distance) scale motions for dense polymeric systems, we have performed dynamic Monte Carlo simulations of chains on a diamond lattice at considerably greater densities than those done previously. Chain dynamics were simulated by a random sequence of three- and four-bond kink motions and end moves. For times shorter than the chain diffusion time, the single bead autocorrelation function  $g(t)$  exhibits three distinct regimes: a short time Rouse-like regime where  $g(t) \sim t^{1/2}$ ; a mid-region where  $g(t) \sim t^\beta$ , followed by a longer time, Rouse-like regime where  $g(t) \sim t^{1/2}$ . There is a smooth crossover from Rouse-like dynamics,  $\beta = 1/2$ , at low density to smaller values of  $\beta$  at higher density, and  $\beta = 0$  at the glass transition density ( $\phi_G = 0.92 \pm 0.01$ ). It is shown that the major motion of the chains is transverse to the chain contour rather than along the chain. The observed motion is successfully analyzed in terms of the motion of defects (holes) through the sample. It is shown that the glass transition at  $\phi_G = 0.92$  is caused by the shutting down of the orientation changing four-bond motions.

## I. INTRODUCTION

In this paper, we examine the local dynamics of polymers packed at high densities. Presumably these are the same motions which persist in the glassy state after the global, long range motions (e.g., overall diffusion) have shut down. Hence, they are of interest in that they determine the relaxational properties of glassy polymers.<sup>1</sup> Since a molecular dynamics simulation is unfeasible for the number of particles and range of time scales necessary for such a study, to obtain a qualitative understanding of these motions, we performed dynamic Monte Carlo (MC) simulations<sup>2</sup> on a model system consisting of chains confined to a diamond lattice where multiple occupancy of lattice sites is prohibited (explicit details of the simulation method will be described in Sec. II). As is well known,<sup>2</sup> a dynamic Monte Carlo simulation is not the solution of an equation of motion but rather is the solution of a Master equation defined by the allowed set of moves and the probabilities of these moves. Thus, we view these simulations as a set of idealized computer experiments from which we extract some general physical features of polymer motions at high density. Since in this preliminary study, we limit ourselves to the short distance (or time scale) motions, nothing presented here has any direct bearing on questions concerning the longer distance diffusive motions, e.g., the adequacy of the reptation model.<sup>3</sup>

In Sec. II, as mentioned above we will present the details of the methodology of our dynamic Monte Carlo simulations. Here we will discuss the allowed moves, the method of chain growth and high density packing, and the equilibration process. Then, in Sec. III we will present the results of the simulations on densely packed polymer chains; concomitantly we will also extract the relevant physical features and show how they can be explained in terms of a simple phenomenological model. This section is subdivided into two

parts. The first deals with the character of the motions themselves. The second shows how these motions provide both a prediction of and explanation for the occurrence of the glass transition in polymers. We conclude in Sec. IV with a brief discussion of our results and their physical implications. Although these results emerge from the study of a particular model system, we expect that the major findings will prove to be more general and robust than the model they came from. Thus, the description of the motional mechanisms will be cast in more general terms.

## II. METHOD

In order to be as physically faithful to the real motions of the carbon backbone of a polymer chain as possible, we have performed the simulation on chains confined to a diamond (tetrahedral) lattice. We did not allow multiple occupancy of lattice sites; hence excluded volume effects (both intra- and interchain) were included as a hard core steric repulsion. No other potential interactions were included; so the simulation represents an athermal, steric repulsion model of a dense polymeric system.

The details of our simulation method are presented in the following order: In Sec. A, we shall describe the dynamic Monte Carlo model we employed, i.e., the allowed moves. In Sec. B, we shall describe the method of growing a dense system of chains. Finally, in Sec. C, we shall describe the equilibration steps and the checks on equilibration made by calculating various static equilibrium properties. Hence a reader interested only in the model and the results can readily skip Secs. B and C and go on to the results described in Sec. III.

### A. Monte Carlo simulation

The diamond lattice is enclosed in a cubic MC box of length  $L$  ( $L$  was always taken to be divisible by 4 for reasons which will be clear below) on a side with periodic boundary conditions. The size of the box  $L$  was chosen to be considerably larger than the root mean square radius of gyration of the chains ( $L = 28$  in most cases, while a bond length, the

<sup>a)</sup> Permanent address: Department of Chemistry, University of Warsaw, 02-093 Warsaw, Poland.

<sup>b)</sup> Alfred P. Sloan Foundation Fellow.

distance between two diamond lattice points, is  $\sqrt{3}$ ). One should recall that due to the openness of the diamond lattice the number of diamond lattice points in an  $L^3$  cubic box is  $L^3/8$ . After the chain growth and equilibration steps described below, the system consists of  $N$  chains each consisting of  $n$  connected lattice sites (we will colloquially refer to  $n$  as the chain length) confined to the MC box. The polymer volume fraction

$$\phi = 8nN/L^3 \quad (1)$$

is the fraction of the occupied lattice sites. For ease of reference, we refer to the occupied lattice sites as beads, the unoccupied sites as holes, and the lattice segment connecting two beads as a bond.

We use the three- and four-bond conformational jumps depicted in Figs. 1(a) and 1(b), respectively, as the basic MC moves. Iwata and Kurata have shown<sup>4</sup> that all motions on a diamond lattice where at least two beads jump can be formed from a sequence of such elemental three- and four-bond jumps. As is apparent from the picture, a three-bond jump only exchanges orientations of the two segments  $G^\pm \rightarrow G^\mp$ . On the other hand, a four-bond jump creates new orientations within the chain. The single possible new orientation of the four-bond unit is randomly chosen from among the three possible orientations of the parallel pair of bonds of the four-bond unit and is accepted if none of the three sites are occupied. At the ends of a chain, we allow one- or two-bond motion of the end beads with the orientation again randomly chosen, as depicted in Figs. 1(c) and 1(d).

In order to completely specify the model, we must not only give the possible moves but also the probabilities assigned to the various moves. Except for a few specific cases which will be discussed separately, we assign the *a priori* probability of a three-bond jump to be 0.3. As we shall show below the results are invariant to this particular choice of *a priori* probability.<sup>5</sup> The ratio of two-bond to one-bond end moves was taken as 2:1.

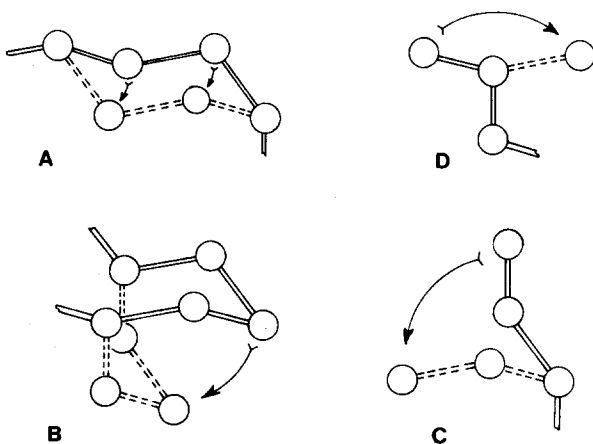


Fig. 1. Elementary conformational jumps for tetrahedral polymers: (a) three-bond motion  $G^\pm \rightarrow G^\mp$ , (b) four-bond motion (with a random choice of the new orientation of the bonds), (c) two-bond motion of end units (with a random choice of the new orientation of the bonds), (d) one-bond motion of end units (with a random choice of the new orientation of the bonds).

The simulation then proceeds as follows:

(i) After the system has been equilibrated, we start with a given spatial configuration of  $N$  chains, all of length  $n$  at a density  $\phi$ .

(ii) We then attempt to move a randomly chosen bead. The type of move is randomly chosen according to the *a priori* probabilities, as is the orientation in the case of four-bond and end jumps.

(iii) If the move is allowed, i.e., the new positions are unoccupied, the move is made. If the move is disallowed, i.e., the new positions are already occupied, we leave the bead at its original position.

(iv) We then repeat steps (ii) and (iii) for another randomly chosen bead and continue until we have attempted on the average to move each bead once, this constitutes one MC time step. That is, a MC time step is the attempt at  $N \times n$  micromodifications (including  $2N$  end moves) of the configuration of the chains. From this new configuration, we then go back to step (ii) to generate the next time step, etc. To enable us to take the desired averages, the configuration at each time step is stored. In addition, to avoid any problems of an initial configuration biasing the results, we repeat the whole procedure over again several times starting with a freshly grown and equilibrated system of chains.

One of the most important average-time dependent properties of the system of densely packed chains which we shall calculate is the single bead autocorrelation function

$$g(t) = n^{-1} \left\langle \sum_{i=1}^n [\mathbf{r}_i(t) - \mathbf{r}_i(0)]^2 \right\rangle, \quad (2)$$

where the averaging is over all of the chains in the system and  $\mathbf{r}_i(t)$  is the coordinate of bead  $i$  at time  $t$ . There is a difficulty with using Eq. (2), as it stands, since the beads at the ends of the chain have considerably higher mobility than those near the middle. This is illustrated in Fig. (2) where we have plotted a representative single bead autocorrelation function for each bead

$$g_i(t) = \langle [\mathbf{r}_i(t) - \mathbf{r}_i(0)]^2 \rangle \quad (3)$$

for a chain of  $n = 98$  at a density of  $\phi = 0.75$ . It is apparent from Fig. 2 where we have plotted  $g_i(t)$  vs  $i$  at a fixed time  $t$  that the increased end mobility is damped out approximately 10 beads in from an end. Hence, since we want our chains to represent the much longer chains of a real polymeric system where end effects are negligible, we shall modify Eq. (2) by eliminating the 10 end beads at each end of the chain from the calculation of  $g(t)$ . Namely,

$$g(t) = (n - 20)^{-1} \left\langle \sum_{i=11}^{n-10} [\mathbf{r}_i(t) - \mathbf{r}_i(0)]^2 \right\rangle. \quad (2')$$

Unless explicitly stated, we shall always use the modified Eq. (2') for the single bead autocorrelation function  $g(t)$ . Other similar correlation functions will be defined below as we have occasion to need them.

## B. Method of growing a dense system of chains

The key to generating a densely packed, amorphous system of chains is to grow them in an initially disordered (quasirandom) configuration. This results in an equilibration step which can be performed in a manageable amount of

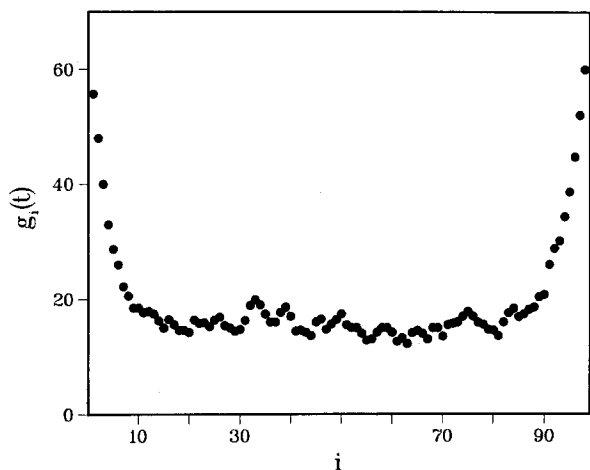


FIG. 2. Individual bead autocorrelation function as a function of bead number  $i$  for a chain of  $n = 98$  at density  $\phi = 0.75$  after an elapsed time of 8250 MC time steps. The average was only over 63 chains so the statistics are not as good as for the other correlation functions.

computer time. A counter example to such a chain growing strategy would be to start with a set of  $N$  trans chains packed in parallel (with folding when necessary) into a regular crystalline structure and where the unoccupied space surrounds the chains up to the edges of the MC box. Clearly for such a high density system, the amount of time necessary to go from such an ordered system to a representative disordered system (if it could be done at all) would be mind boggling.

The chain growing algorithm we used is a necessary compromise between growing the chains quickly so that the amount of computer time is reasonable, and growing the chains slowly enough that they can equilibrate as much as possible during the growth stage (with a consequent saving of computer time during the subsequent equilibration step). There is a degree of arbitrariness in the algorithm described below, as will become apparent; however, these arbitrary features were chosen with the above compromise in mind. Furthermore, we have checked that these arbitrary procedures have no effect on the "measured" properties of the equilibrated system.

The algorithm for the semisimultaneous growth of the chains is:

(1) The  $N$  chains are initiated at  $N$  random lattice positions modulo 4 in our MC box. That is we chose  $N$  random positions in a box  $(L/4)^3$  and then multiplied all the coordinates by four. This avoids very close clustering of initiation points.

(2) We always pick the chain we will attempt to modify by using a random permutation algorithm.

(3) We attempt to grow (propagate) the chain by adding a bead (a bond) in a random orientation at one of the chain ends (which is also chosen randomly). Of course, we avoid multiple occupancy of lattice sites.

(4) When the average size of the chains reaches six beads, we then shift over to a combined propagation, reptation, and kink motion algorithm. A reptation step is achieved by clipping a bead off one end of the chain (chosen randomly) and adding it on to the other end in a random orientation (if a hole exists at the desired lattice point). The

kink motions refer to the set of MC moves (and *a priori* probabilities), i.e., three- and four-bond jumps and end moves discussed in Sec. II A and depicted in Figs. 1(a)–1(d). Combining these sets of moves with the chain propagation step allows the chains to move and relax as they are growing. The combined algorithm is:

(a) We continue to pick the chain that will undergo micromodification by using the random permutation algorithm as in step (2) above.

(b) If for the chain picked,  $n_i(t) < \bar{n}_i(t)$ , where  $n_i(t)$  is the length of the chain in question and  $\bar{n}_i(t)$  is the average length of chains at that time  $t$  in the chain growing process, we attempt to initiate a chain propagation step.

(c) If (b) is satisfied, we randomly decide whether to attempt a chain propagation step with an *a priori* probability of 1/2. While 1/2 is clearly arbitrary, this step serves to slow down the chain growth to allow for equilibration.

(d) If step (c) results in chain propagation, then we randomly pick an end and affix a new bead to it whose bond is randomly oriented. Again for the propagation attempt to be successful, it must not violate the prohibition against double occupancy of lattice sites.

(e) If step (c) results in the failure to propagate the chain, we attempt a reptation step, again subject to the double occupancy restriction.

(f) We then attempt to perform the kink motions on the chain in question. Both one- and two-bond end chain jumps are tried as described in Sec. II A.

(g) The interior three- and four-bond jumps are also performed as in Sec. II A except that the decision over whether to initiate an internal jump attempt for a particular bead is made with an initial *a priori* probability of between 0.1 and 0.2. This is again a somewhat arbitrary attempt to increase the amount of equilibration during the chain growth process.

(h) We continue to sample the chains using the random permutation algorithm. When we come to the point where the chain picked has a length  $n_i(t) = n$ , the desired chain length, we omit the chain propagation steps (b)–(d) and go directly to the reptation step (e).

(i) We continue the procedure until all chains are length  $n$ . We are then ready for the equilibration step.

### C. Equilibration

The equilibration procedure we used is: (1) As we step through the chains, for each chain we attempt a reptation step as described in Sec. II B. (2) We then attempt to move the bead in the chains using the three- and four-bond jumps and end moves as described in Sec. II A. One complete cycle through all of the chains in the system constitutes an equilibration time step. It should be noted that the reptation move is a much more efficient move for equilibration than the three- and four-bond jumps. That is, it relaxes configurations faster since it allows the chains to sample a greater amount of configuration space more quickly.<sup>6</sup>

Of course as the density increases, the fraction of allowed moves goes down and the equilibration time increases. In order to speed up the equilibration process at higher densities, we modify step (1) for  $\phi > 0.75$  to:

(1') For part of the equilibration time, we put a small drift on the reptation by biasing the *a priori* probability in a particular, but arbitrary, direction. We then shift the drift bias and repeat the drift procedure in a different direction. Otherwise the procedure is the same as above. This modification in the equilibration procedure allows chains to more easily escape from trapped configurations.

The time necessary for equilibration is relatively short due to the chain growing procedure we have used. For example for a short chain where  $n = 25$  at a medium density  $\phi = 0.5$ , equilibration is complete in  $\sim 10^3$  equilibration time steps. The time obviously increases with increasing density and even more with increasing chain length. For example, at  $n = 147$ , the longest chain length used in this study and  $\phi = 0.75$ ,  $\sim 10^6$  time steps are required for equilibration.

Of course, one can never *prove* that an equilibrated system has been achieved; however, before trusting the results for the dynamics, as a minimum one should use various tests to check whether the static properties are properly described.

We used both internal and external checks. One such internal check is that the ratio of allowed to attempted three- and four-bond jumps had to remain constant with time and not drift as they do for incompletely equilibrated samples. Furthermore, these ratios had to be the same for different runs (i.e., different chain growth and equilibration steps) at the same chain length and density. In addition, the ratio of *trans* to *gauche* configurations had to be the statistically correct value, which they were to within 1% for the size of the systems studied.

A further check is given in Table I where we present the hole clustering probability for  $n = 98$  chains packed at various densities. It is apparent from line two of each entry in this table, that the mean field results get worse as density increases as would be expected.<sup>7</sup> Moreover, looking at the third line in each entry we see that the conditional probability of adding a new hole to an already existing cluster of holes remains essentially constant at a given density (making due allowances for the poorer statistics at higher densities and larger cluster sizes) as it must.

External checks on equilibration were done by checking static expectation values with previously calculated values.

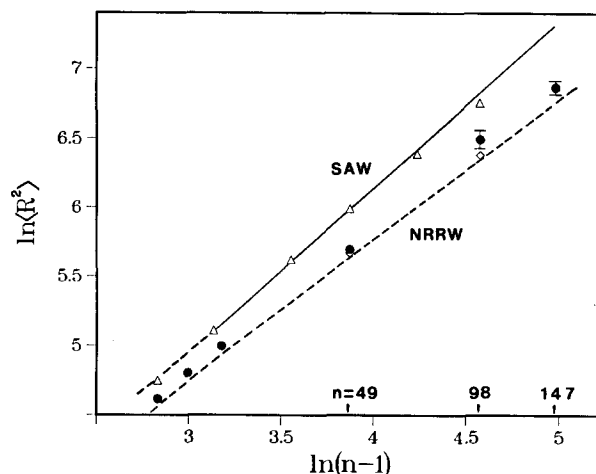

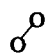
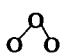
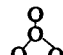
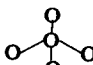


FIG. 3. Mean square end-to-end separation  $\langle R^2 \rangle$  as a function of chain length ( $n$ ) at various concentrations. The self-avoiding walk solid line (SAW) was taken from the MC calculation in Ref. 8, while the nonreversal random walk dashed line (NRRW) was taken from Ref. 9. The triangles are for a single chain in the MC box (except for the two longest chains with  $n = 70$  and  $98$  which have two chains in the MC box). The black dots are for  $\phi = 0.75$  and the diamonds are for  $\phi = 0.8214$ . The error bars are the standard deviation for a single run. Where no error bar is shown, the error is less than the size of the symbol.

An example of this is given in Fig. 3. Here we show the mean squared end-to-end separation for the chain as a function of chain length for various densities. The low density results (which are not really the subject of this paper but were calculated to check the methodology) lie on the theoretical self-avoiding walk random (SAW) curve,<sup>8</sup> as they should. Similarly, the high density results lie on the curve obtained from the second-order, nonreversing random walk theory (NRRW), of Domb and Fisher.<sup>9</sup> More detailed analysis of the concentration dependence of the coil dimensions are presented for a chain length  $n = 49$ . In Fig. 4, we plot the mean square end-to-end distance  $\langle R^2 \rangle$  and the fourth reduced moment of the distribution of the end-to-end vector  $\sigma(4,2) = \langle R^4 \rangle / \langle R^2 \rangle^2$  vs volume fraction of polymer  $\phi$ . With increasing  $\phi$ , the size of the polymer coil decreases monotonically and approaches, in the bulk density limit, the theoretical value for an NRRW consisting of  $n - 1 = 48$  bonds. Meanwhile,  $\sigma(4,2)$  increases from the value for SAW's at infinite dilution to the value for NRRW at very high concentration. These results extend the findings of previous MC simulations of three dimensional, monodisperse

TABLE I. Statistics of hole clusters in a diamond lattice system. Chain length  $n = 98$ .

Type of "clusters"		$\phi = 0.25$	$\phi = 0.5$	$\phi = 0.75$	$\phi = 0.8214$
1. 	$P(1)$	0.75	0.5	0.25	0.178
	$P(1)/(1 - \phi)$	1.0	1.0	1.0	1.0
2. 	$P(2)$	0.646	0.3324	0.1014	0.0558
	$P(2)/(1 - \phi)^2$	1.148	1.330	1.622	1.749
	$P(2)/P(1)$	0.859	0.665	0.400	0.314
3. 	$P(3)$	0.556	0.2241	0.04020	0.01526
	$P(3)/(1 - \phi)^3$	1.313	1.793	2.573	2.679
	$P(3)/P(2)$	0.860	0.674	0.396	0.273
	$P(4)$	0.481	0.1503	0.01576	0.00393
4. 	$P(4)/(1 - \phi)^4$	1.519	2.404	4.035	3.865
	$P(4)/P(3)$	0.864	0.670	0.392	0.258
	$P(5)$	0.414	0.0995	0.005753	0.00112
5. 	$P(5)/(1 - \phi)^5$	1.744	3.183	5.861	6.174
	$P(5)/P(4)$	0.861	0.662	0.365	0.285

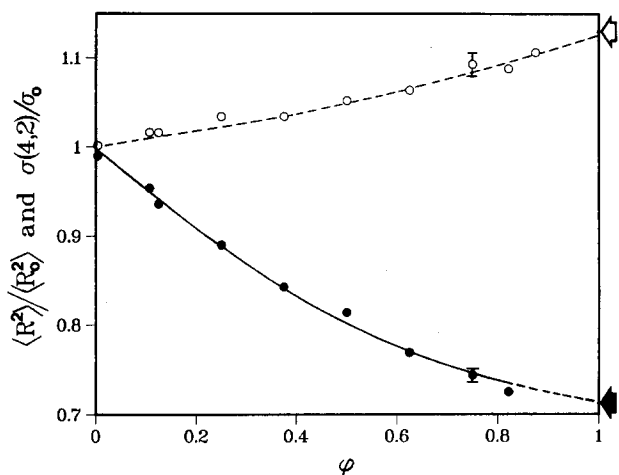


FIG. 4. The mean square end-to-end separation  $\langle R^2 \rangle$  and the fourth reduced moment,  $\sigma(4,2) = \langle R^4 \rangle / \langle R^2 \rangle^2$  as a function of density  $\phi$  for chain length  $n = 49$ . In both cases we have normalized the result to the value at zero density.  $\langle R_0^2 \rangle$ , the mean square end-to-end separation at  $\phi = 0$ , is 400.3.  $\sigma_0$ , the fourth reduced moment at  $\phi = 0$ , is 1.4313. The arrow corresponds to the result of the NRRW theory of Ref. 9.

polymer systems<sup>10</sup> to considerably longer chains and could be taken as proof of appropriate equilibration of our model systems. For the longer chains we studied ( $n = 98$  and  $n = 147$ ), similar behavior was observed; however, the scattering of the data for  $\langle R^2 \rangle$  and  $\sigma(4,2)$  at high density is greater.

### III. RESULTS

This section is divided into two subsections, the first discusses the nature of the short time motions and the second discusses the onset and origin of the glass transition.

#### A. Short distance motions

In Fig. 5 we show a log-log plot of the single bead autocorrelation function at a density  $\phi = 0.75$ . It is apparent that there are three distinct regimes.<sup>11</sup> At short times  $g(t) \sim t^{1/2}$ , characteristic of Rouse-like dynamics.<sup>12</sup> The middle time regime is characterized by  $g(t) \sim t^\beta$ , where  $\beta = 0.33$  for

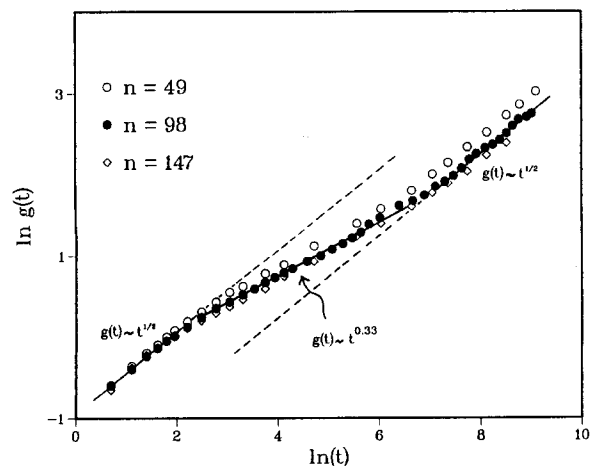


FIG. 5. Single bead autocorrelation function as a function of time for various chain lengths at a density  $\phi = 0.75$ .

this density. The third regime is again Rouse-like in the sense that  $g(t) \sim t^{1/2}$ . At still longer times not shown in Fig. 5 and not germane to the subject of this paper,  $g(t) \sim t$ . This is the time regime characteristic of diffusional motion of the chain as a whole and will not be discussed further here.

Figure 5 also shows the chain length dependence of  $g(t)$ . While the results for  $n = 49$  are clearly different from the others, the results for  $n = 98$  and 147 are nearly coincident throughout the first  $t^{1/2}$  region, the  $t^\beta$  region and perhaps into the onset of the second  $t^{1/2}$  region. These are the regions we will be interested in this paper, and it appears that both qualitatively and quantitatively we have reached asymptotia with respect to chain length for describing the motions in this time regime. Thus we feel justified in using chains of  $n = 98$  to study the density dependence of the motions which is the major focus of the rest of the paper. Moreover, the fact that we are examining a region where the motion becomes independent of chain length indicates that this regime is probing local motions of the chain rather than overall chain movement.

Before any further discussion of the various time regimes shown in Fig. 5 and their density dependence given in Fig. 6, we must investigate the types of motions we are probing. However, before doing so, there is a loose end that must be cleared up. In Sec. II A, we stated that the results of the simulation were invariant to the choice of *a priori* probabilities for the three- and four-bond jumps. Figure 7 presents a log-log plot of  $g(t)$  vs  $t$  for  $n = 98$ ,  $\phi = 0.75$  and using three different *a priori* probabilities of three-bond jumps, 0.15, 0.30, and 0.65. As can be clearly seen the results are insensitive to the choice of *a priori* probability. The reason for this is that in a dense system most of the attempted moves are unsuccessful, either because there are no vacancies to jump into or because the chain in question is not in a configuration

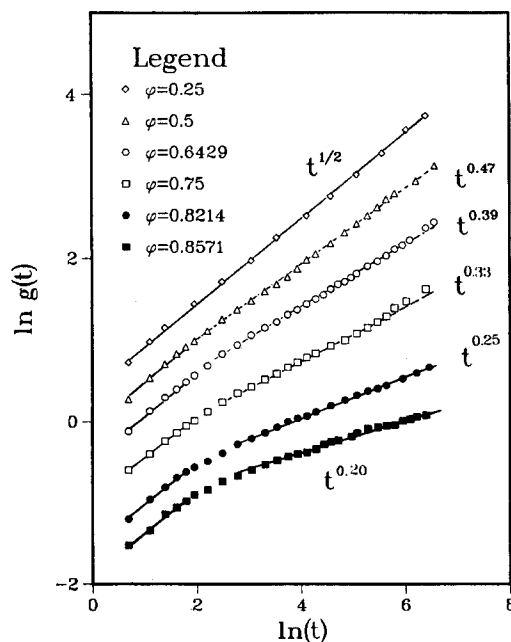


FIG. 6. Single bead autocorrelation function as a function of time for several densities at a chain length  $n = 98$ . The time dependence of the  $t^\beta$  regime (see the text) is listed for each curve.

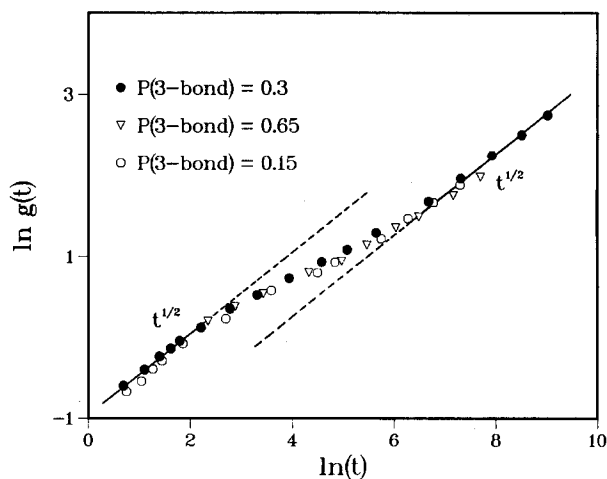


FIG. 7. Single bead autocorrelation function as a function of time for several different values of the *a priori* probability of three-bond jumps (see the text) for a chain length  $n = 98$  and a density  $\phi = 0.75$ .

allowed to move into the available vacancies. Hence, the system itself determines the fraction of three- and four-bond jumps, independent of our choice. In fact for the three cases depicted in Fig. 7 the fraction of accepted three-bond moves was 0.077 with differences in the next significant figure. Hence unless something drastic is done to the *a priori* probabilities, the results are independent of the choice.

The next question we address is what is the nature of the chain motion? Is the motion down the chain, i.e., along the chain contour ( $c$ ), or transverse to the chain, i.e., across the sample ( $s$ )? To this end, Figs. 8 and 9 present log-log plots of the mean square displacement of correlated elementary conformational jumps across the sample ( $g_s$ ) and down the chain ( $g_c$ ), respectively vs time at several densities for chains of  $n = 98$ . In Table II, we give the conformational jump statistics along the chain and across the sample, again for  $n = 98$  as a function of density. Examining Figs. 8 and 9 we see that the mean-square-jump displacement possesses three time regimes, exactly analogous to the three regimes in

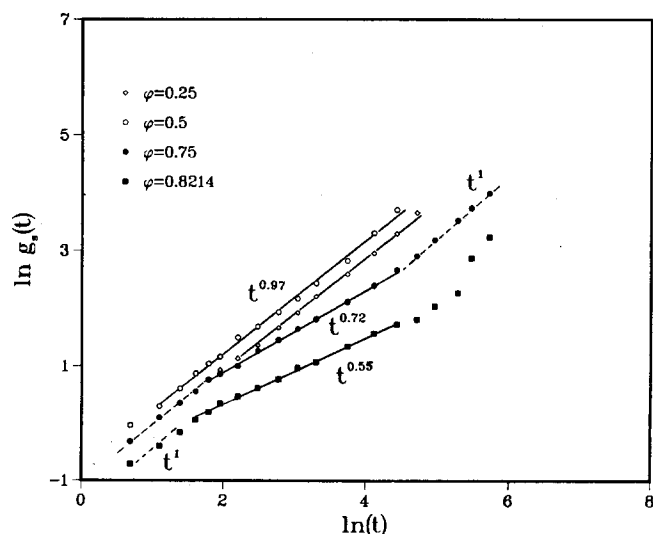


FIG. 8. The mean square displacement of jumps across the sample as a function of time for several concentrations at a chain length  $n = 98$ . The time dependence of the  $t^\alpha$  regime (see the text) is given for each curve.

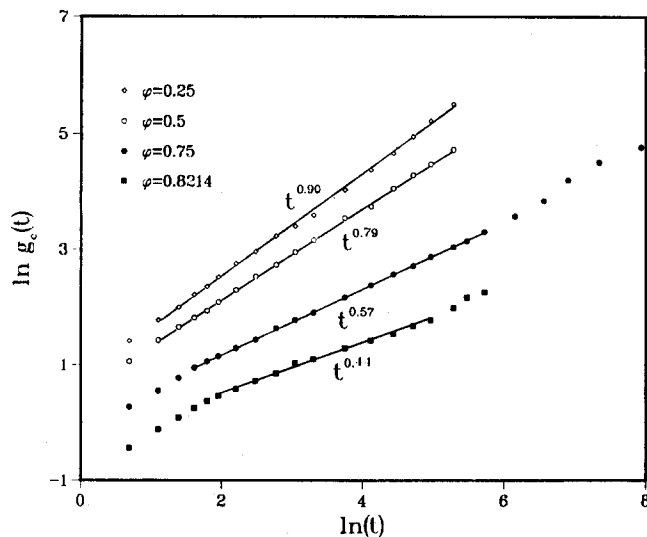


FIG. 9. The mean square displacement of jumps down the chain as a function of time for several concentrations at a chain length  $n = 98$ . The time dependence of the  $t^\alpha$  regime (see the text) is given for each curve.

the single bead autocorrelation function—a short time  $t^{-1}$  regime, a middle time  $t^\alpha$  regime and a longer time, second  $t^{-1}$  regime. However the middle regime has a larger value of  $\alpha$  (for the same value for  $\phi$ ) for motion across the sample than for motion down the chain. Thus, the jumps move faster across the sample than they move down the chain. By comparing columns 2 and 3 of Table II we see that the probability of a jump across the sample is larger than the probability of a jump down the chain. Hence, since there are more jumps going faster transverse to the chain than along the chain, we conclude that the dominant motion is transverse to the chain and across the sample.

To aid in the visualization of the transverse motion we show two representative, before and after “snapshots” of the motion of one of the chains in a dense system of chains of  $\phi = 0.75$  in Figs. 10 and 11 for  $n = 49$  and 98, respectively. In both figures the time is sufficiently long that the mean displacement of a single bead is on the order of the radius of gyration, so that one can see appreciable net displacement, and is well into the second  $t^{1/2}$  regime of the single bead correlation function, see Fig. 5. In Fig. 10 we show the snapshots for a shorter chain,  $n = 49$ , where, since the picture is less cluttered, it is somewhat easier to see the relative motion. Figure 11 shows the same sort of before and after snapshots for the more representative  $n = 98$  chain. It is apparent on looking at these pictures (and we have examined many more) that relatively large parts of the chain have moved a long distance in a direction on the average perpendicular to the local chain axis. However the positions of several of the beads (see in particular Fig. 11) have remained unchanged. In fact a detailed examination of the time trajectory shows the number of immobile beads has decreased but a few such fixed beads remain over the entire course of the second Rouse-like regime. Hence we cannot yet be in the true global diffusion regime [ $g(t) \sim t$ ].

The physical reason that the major motion is across the sample rather than down the chain is quite easy to understand. In order for a chain to undergo a jump, it must be in a

TABLE II. Statistics of correlated conformational jumps for chains with  $n = 98$ -jump propagation probability<sup>a</sup>.

$\phi$	Down the chain	Across the sample	$f_{i,j}$ reverse jump	Conditional probability	
				$p(s,c)^b$	$p(c,s)^c$
0.25	0.335	0.585	0.080	0.377	0.532
0.50	0.216	0.703	0.081	0.277	0.655
0.75	0.193	0.683	0.124	0.289	0.623
0.8214	0.189	0.668	0.143	0.320	0.572

<sup>a</sup>Total probability of a correlated jump, sum of columns two, three, and four is unity.

<sup>b</sup>Probability that an observed cross sample succession of jumps was preceded by a jump propagating down a chain.

<sup>c</sup>Probability that an observed succession of jumps down the chain was preceded by a jump propagating across the sample.

configuration in which such a jump is possible and it must have vacancies to jump into. For example, the middle of a stretch of an all-*trans* conformation cannot perform a three-bond jump. In addition, a three-bond jump requires two adjacent holes to jump into, while a four-bond jump requires three adjacent holes. Once a chain has for example undergone a three-bond (two-hole) jump, it leaves two holes in its formerly occupied position. Hence whether the adjacent chain can now also undergo a three-bond jump depends only on whether its conformation will allow such a jump and not on the availability of two holes to jump into. On the other hand, the occurrence of another three-bond move in the same chain and adjacent to the first one requires another set of two holes as well as the correct conformation. Hence the probability of two successive cross-sample three-bond jumps is proportional to  $p(2)$ , where  $p(2)$  is the probability of having a two hole cluster (see Table I) while the probability of having two successive jumps down the chain is proportional to  $p(2)^2$ . Since from Table I,  $p(2)$  is a small number at high densities, the motion is much greater in the transverse direction. Similar considerations hold for four-bond jumps.

Hence we have the picture of successive jumps moving from chain to adjacent chains, essentially perpendicular to the local chain axis.

It is easier to visualize the motion by focusing on the complementary motion of clusters of holes randomly moving through the sample rather than focusing on the chain motion directly. However, a note of caution must be invoked when thinking of the motion as hole motion. Since a hole cluster can only jump when a chain has jumped, the motion of the hole clusters has topological constraints imposed on it by chain connectivity. Hence, the motion of the hole clusters, while random, is highly constrained and not at all like the free diffusion of defects in "normal" (i.e., small molecule) crystalline solids. Keeping this cautionary note in mind (and we shall have to make use of it later) we have the picture of clusters of holes diffusing through the sample and moving locally perpendicular to the chain axis. Single holes can only contribute to end motion so they do not move far on their own. Two-hole clusters move by three-bond jumps, three-hole clusters can move by four-bond jumps or they can be split up by a three-bond jump into a two-hole cluster and

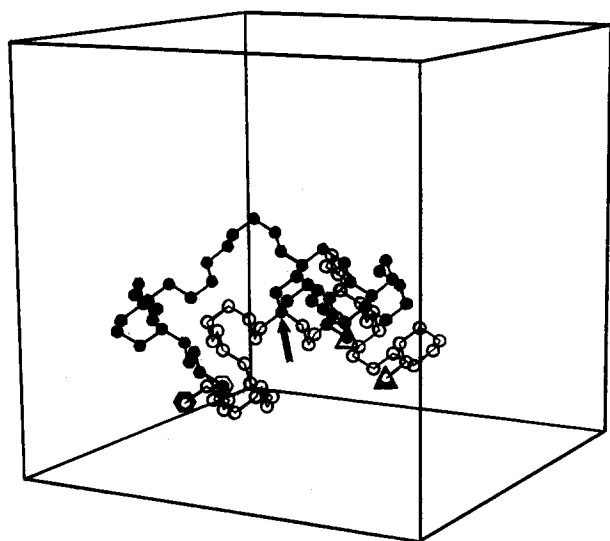


FIG. 10. Two superimposed snapshots of a polymer chain of length  $n = 49$  separated by 20 000 MC time steps. This simulation was at a density  $\phi = 0.75$ . An arrow points to an example of a bead which has not moved during the time course of the simulation. The two ends of the chain are shown by a triangle and a hexagon.

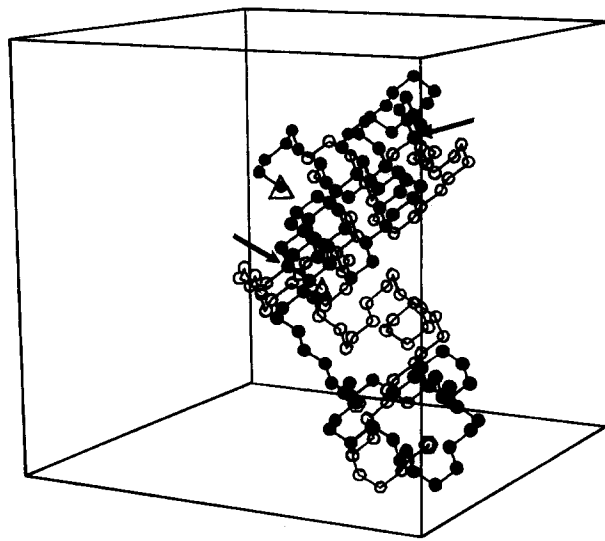


FIG. 11. Two superimposed snapshots of a polymer chain of length  $n = 98$  separated by 45 000 MC time steps. This simulation was at a density  $\phi = 0.75$ . Arrows point to two examples of a bead which has not moved during the time course of the simulation. The two ends of the chain are shown by a triangle and a hexagon.

an immobile single hole. A single hole can only become mobile by coalescing with a two-hole cluster to become a three-hole cluster. Jumps down the chain are caused by a succession of hole clusters passing for the most part through the chain.

Utilizing this picture of hole clusters jumping (diffusing) through the sample, we are now in a position to analyze and understand the various time regimes in the single bead autocorrelation function. At short times, we see clusters of holes, mostly two-hole clusters (see Table I) diffusing across the chain axis jumping from chain to chain. Such a diffusion of hole clusters exhibits the standard diffusive linear proportionality of the mean square displacement on time. This is the origin of the first linear time regime exhibited in Fig. 8. As is well known,<sup>13</sup> a defect diffusion description (in this case a hole cluster) causes a Rouse-like  $t^{1/2}$  dependence for the single bead correlation function as exhibited in Figs. 5 and 6.

However, a two-hole cluster cannot diffuse very far before it runs into a segment of chain that due to its configuration is unable to undergo a three-bond jump. One example, of many such configurations, would be an all-*trans* stretch. The only thing that the two-hole cluster can do is diffuse back in the direction it came from, until it runs into another chain conformation which cannot undergo a three-bond flip. Thus we have a picture of two-hole clusters diffusing across the chains and constrained within a box by chain conformational restrictions. These configurational barriers to two-hole diffusion can be relaxed, but this requires configuration changing four-bond jumps. That is, in the hole cluster picture, it requires the passage of a three-hole cluster (or perhaps several three-hole clusters). Since three-hole clusters are relatively rare in dense systems (See Table I) the time scale for the destruction of a barrier to two-hole motion is long compared to the two-hole diffusion (or jump) time. Of course, the passage of a conformation changing three-hole cluster not only destroys configurational barriers but also creates new ones. Thus, the two-hole cluster now finds itself confined to a new configurational box in which it can diffuse until the configurational constraints relax following the passage of another three-hole cluster.

We have schematically illustrated this process in Fig. 12. The two-hole cluster is constrained in a conformational box of average length  $l$  with reflecting walls. Within this box, it undergoes Brownian diffusion. The cluster can also hop from box to box with a rate constant  $k$  which denotes the rate of configuration changing jumps. As mentioned above, the short time (i.e., short compared to the mean time to traverse the box) mean-square-hole displacement is proportional to  $t$  with a proportionality constant reflecting the diffusion con-

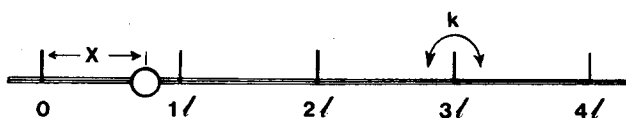


FIG. 12. A schematic illustration of the "box model" (see the text) for the diffusion of two-hole clusters. The average length of the conformational box is  $l$  within which the hole clusters freely diffuse with a diffusion constant  $D$ . The rate of hopping from one box to another is given by  $k$ . The kinetic diffusion equation for this model is given in Eq. (4).

stant (or rate of three-bond jumps). At long times as shown in Fig. 8, the behavior of the two-hole cluster is again diffusional with a mean square displacement again proportional to  $t$  and the proportionality constant reflects the box hopping rate constant (i.e., the rate of configuration changing four-bond jumps). This long time defect diffusion regime again produces a second Rouse-like  $t^{1/2}$  regime for the single bead correlation function such as is shown in Fig. 5.

The intermediate time regime is a pausing regime where the two-hole clusters have felt the effects of the configurational barriers but not enough time has passed for configurational changing four-bond jumps. As the density increases, the number of three-hole conformation changing clusters decreases as shown in Table I, hence the pausing time increases. This is reflected in the decreasing slope for the intermediate time regime with increasing density for the jump mean square displacement shown in Figs. 8 for  $g_s(t)$  vs  $t$  and in the single bead correlation function of Fig. 6.

A mathematical realization of the model illustrated in Fig. 12 is given by the kinetic diffusion equation

$$\frac{\partial \rho_i(x,t)}{\partial t} = D \frac{\partial^2 \rho_i(x,t)}{\partial x^2} - 2k\rho_i(x,t) + k[\rho_{i+1}(x+l,t) - \rho_{i-1}(x-l,t)], \quad (4)$$

where  $\rho_i(x,t)$  is the probability that the two-hole cluster is located at position  $x$  within box  $i$  at time  $t$ ,  $D$  is the diffusion constant for motion within the box and  $k$  is the rate at which it jumps from out of box  $i$  a distance  $l$  (the box length) into an adjacent box. Solving Eq. (4) using the reflecting boundary condition at the walls of the box, we can use the probability to obtain the mean square displacement

$$\langle \Delta x^2(t) \rangle = 2kt + 1/6 - \frac{16}{\pi^4} \sum_{m=0}^{\infty} \frac{\exp\{-[(2m+1)^2 D \pi^2 / l] t\}}{(2m+1)^4}. \quad (5)$$

The formalism embodied in Eqs. (4) and (5) carries over to the down chain autocorrelation function of jumps,  $g_c(t)$ , if we identify the  $\rho_i(x,t)$  as the probability of a conformational jump at position  $x$  in the  $i$ th box of length  $l$ . The down chain motion is caused essentially by a succession of cross-chain holes which allows the elemental jumps to propagate on the average a distance  $l$  before coming to an configurational barrier. This barrier is then relaxed by conformational changes with a rate constant  $k$ .

We have fit Eq. (5) to the simulation results depicted in Figs. 8 and 9. The phenomenological parameters of this simplified box-jump diffusion model are given in Table III along with the standard deviation of the fit for a variety of densities. While  $D$ , the short distance hole diffusion constant, and  $l$ , the average distance between configurational barriers, decrease with increasing density,  $k$ , the rate at which conformational barriers are relaxed, decreases much more rapidly at high density. This is because ratio of four-bond (conformation changing) jumps to three-bond (conformation preserving) jumps decreases with increasing density. This will be discussed in greater detail in the next subsection.



TABLE III. Fit of box diffusion model<sup>a</sup> to  $g_s(t)$  and  $g_c(t)$ .<sup>b</sup>

$\phi$	Down the chain				Std <sup>c</sup> deviation	Across the sample			Std <sup>c</sup> deviation
	$k$	$l$	$D$			$k$	$l$	$D$	
0.25	0.58	8.3	0.053	0.13	...	...	...	...	
0.5	0.27	8.4	0.056	0.09	...	...	...	...	
0.75	0.34	6.5	0.043	0.10	0.076	3.8	0.034	0.07	
0.8214	0.010	4.4	0.035	0.09	0.019	3.6	0.034	0.04	

<sup>a</sup>Equation (5).

<sup>b</sup>See Figs. 8 and 9.

<sup>c</sup>This is the standard deviation of a point on a plot of  $\ln g(t)$  vs  $\ln t$  as given in Figs. 8 and 9.

## B. The glass transition

The kinetic description of the glass transition we shall adopt is that at the glass transition long distance motions shut down. That is, above the glass transition, on an experimental time scale long distance diffusive motions are observable. Below the glass transition, due to kinetic frustrations, the long distance, diffusive type motions no longer occur. This is the type of description that has emerged from recent theoretical studies of simple glassy systems.<sup>14,15</sup> Here we want to investigate what kinds of motions are involved in the shutting down of the long distance motions in polymer glasses.

From the description we have constructed in the previous subsection, it is evident that if there were no configuration changing four-bond jumps, diffusion of the two-hole clusters would be constrained to their short distance configurational box. Hence, there should be no long distance diffusional motion of the chains.

We checked this by doing a computer experiment and performed a simulation on chains of  $n = 98$  at a density of 0.75 where we set the *a priori* probability of four-bond jumps to zero. The results of this simulation are presented in Fig. 13 as a log-log plot of the single bead autocorrelation function vs time. We see that beyond the Rouse-like  $t^{1/2}$  regime the correlation function now has a plateau. The chains can-

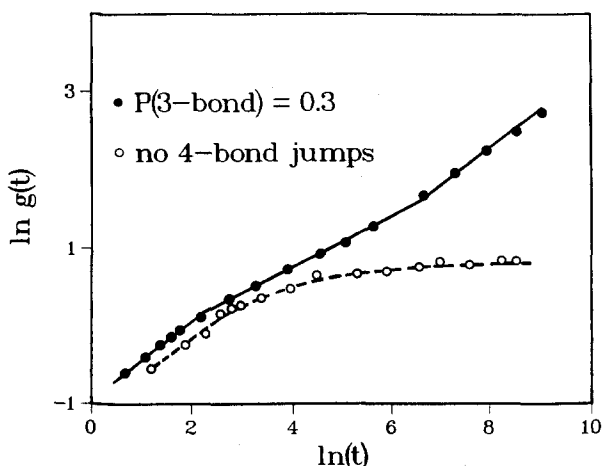


FIG. 13. The single bead autocorrelation function as a function of time, where no four-bond jumps were allowed, showing a glass-like behavior. For comparison we have also plotted the autocorrelation function where four-bond jumps were allowed showing a normal liquid-like behavior. Both simulations were done for chains of length  $n = 98$  at a density of  $\phi = 0.75$ .

not move over long distances in the absence of configuration changing, four-bond jumps. For short times, however, the correlation function is the same as when the four-bond motions are included.

Based on the above, we now propose that the glass transition can be described by a free-volume theory very much like that originally proposed by Fox and Flory<sup>16</sup> (and many people since).<sup>17</sup> When the density gets high enough (i.e., the free volume gets small enough) the probability of having three-hole clusters is sufficiently small that there are no longer any configuration changing jumps, and the long distance motions shut down. Hence, we can find the density of the glass transition by extrapolating our simulation data to the point where the four-bond motions have shut down. In Fig. 14, we plot the ratio of accepted four-bond jumps to accepted three-bond jumps vs  $\ln(1 - \phi)$ . The extrapolated straight line goes to zero at a predicted  $\phi_G = 0.92 \pm 0.01$ .

This prediction for  $\phi_G$  is the same as was found in a diamond lattice Monte Carlo simulation by Batie, Viovy, and Monnerie.<sup>18</sup> They did a simulation for chains of  $n = 32$  (with one short chain added to the MC box to obtain the desired density) and found that the single bead correlation function flattened out, just as in Fig. 13, for a density between 0.910 and 0.918. They did not, however, present any analysis of the kinds of motions which freeze out and thus produce the glass transition.

While experimental estimates of the free volume neces-

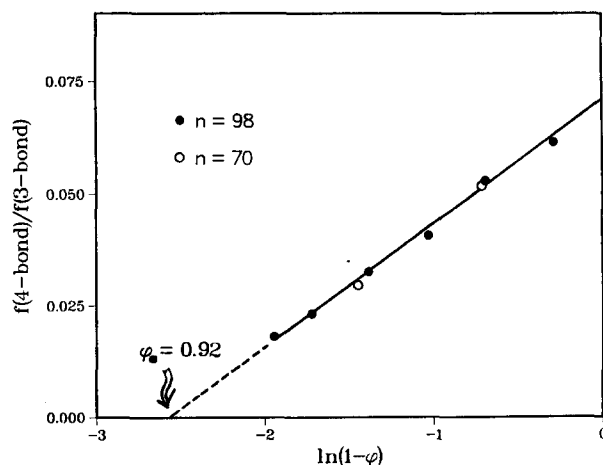


FIG. 14. The ratio of accepted four-bond jumps to accepted three-bond jumps as a function of  $\ln(1 - \phi)$ . This fraction extrapolated to zero gives a predicted  $\phi_G = 0.92 \pm 0.01$ .

sary to have a glass transition are somewhat fuzzy (since free-volume itself is a fuzzy concept, in that it can be defined in a number of ways), our theoretical estimate of 8% free volume for the glass transition is not inconsistent with the experimental results.<sup>19</sup>

#### IV. DISCUSSION

Using densely packed chains on a diamond lattice as a model system to investigate the properties of dense polymeric systems, we have been able to arrive at a simple general picture for the short time dynamics and the onset of the glass transition. It remains, however, to ascertain whether, and in what way, the diamond lattice Monte Carlo system is a reasonably faithful zeroth-order physical model for real, dense, polymeric systems. The ultimate answer to this question must await the completion of a large amount of computational experiments, real experiments, and analytical theory. However, one indication that Monte Carlo simulation of polymer dynamics on a diamond lattice is not completely nonphysical, is that preliminary calculations<sup>20</sup> in the longer time diffusive regime give a molecular weight dependence of the diffusion constant in reasonable agreement with the experimental value<sup>21</sup> of  $n^{-2.1}$ .

We conclude by casting the major findings of this model study into a lattice independent language which should have a wider validity than just the model system examined here.

If we subdivide the basic local motional transitions of a polymer chain into two classes: those which conserve configurations, and those which change configurations, the configurational changing class of motions require a larger local free volume than those which conserve configurations. On the shortest distance scale, the motion of a dense system of polymer chains consists mainly of configuration preserving transitions and is transverse to the local chain axis. The motion on this short distance scale can be pictured as random diffusion of small free volume defects (or holes) across the sample, subject to the topological constraints imposed by the chain connectivity and configurations.<sup>22</sup> This "free" diffusion of holes runs into configurational barriers caused by chain topologies that cannot undergo configuration preserving transitions. Hence the hole mobility is constrained by the chain topology. In order to release this constraint, a larger, but still local, density fluctuation is required which creates enough free volume to enable the constraining chain to undergo a configuration changing local transition (or perhaps transitions). It is these local free volume fluctuations, that allow for configuration changes, which act as the gating mechanism for longer distance scale diffusion of free volume and allows the longer distance and time scale motions.

When the free volume of the system becomes small enough, these local free volume fluctuations shut down. Hence the configuration changing transitions can no longer occur. With no mechanism available to release the configurational barriers, the hole motion is now locally trapped, and hence there are no long distance, diffusive motions of the polymer chains. It is the shutting down of these local free volume fluctuations which signals the onset of the glass tran-

sition. It is not that local density fluctuations no longer occur below the glass transition, but rather that the density fluctuations that do occur do not create enough free volume to allow configuration changing transitions.

The idea that the glass transition can be understood in terms of free volume, as we have already indicated, is of course by no means new. What is new is that we have for the first time shown a specific realization of the ideas that have been around for a long time. Moreover, we have shown that one can shut down the long distance motion by shutting down a local motion that allows the long distance motion to occur. This local configuration changing motion acts as a gate for the long distance motions and comes naturally out of the picture necessary for understanding the short time motion of dense polymeric systems and is not grafted on as an afterthought to describe the glass transition. Thus the description of the motions is a consistent one.

#### ACKNOWLEDGMENTS

This work was supported in part by grants from the National Science Foundation Polymer Program and the Petroleum Research Fund administered by the American Chemical Society. The authors would like to thank Professor Bruno Zimm for a very helpful pre-seminar conversation.

<sup>1</sup>J. D. Ferry, *Viscoelastic Properties of Polymers* (Wiley, New York, 1980).

<sup>2</sup>A recent review on dynamic Monte Carlo simulations for polymer systems with references to earlier work is A. Baumgartner, *Annu. Rev. Phys. Chem.* **35**, 419 (1984).

<sup>3</sup>P. G. de Gennes, *Scaling Concept in Polymer Physics* (Cornell University, Ithaca, New York, 1979).

<sup>4</sup>K. Iwata and M. Kurata, *J. Chem. Phys.* **59**, 6119 (1973).

<sup>5</sup>Similar results were also shown by K. Kremer, *Macromolecules* **16**, 1632 (1983).

<sup>6</sup>F. T. Wall and F. Mandel, *J. Chem. Phys.* **63**, 4592 (1975).

<sup>7</sup>See, e.g., A. Bellemans and E. De Vos, *J. Poly. Sci. Symp.* **42**, 1195 (1973); H. Okamoto, *J. Chem. Phys.* **64**, 2686 (1976); A. Kolinski, *J. Polym. Sci. Polym. Lett. Ed.* **22**, 407 (1984).

<sup>8</sup>P. J. Gans, *J. Chem. Phys.* **42**, 4159 (1965).

<sup>9</sup>C. Domb and M. E. Fisher, *Proc. Cambridge Philos. Soc.* **54**, 48 (1958).

<sup>10</sup>J. G. Curro, *Macromolecules* **12**, 463 (1979).

<sup>11</sup>Somewhat similar time regimes and density dependencies were found in a recent MC simulation for a cubic lattice by C. C. Crabb and J. Kovac, *Macromolecules* **18**, 1430 (1985).

<sup>12</sup>P. E. Rouse, *J. Chem. Phys.* **21**, 1272 (1953).

<sup>13</sup>See, e.g., K. E. Evans and S. F. Edwards, *J. Chem. Soc. Faraday Trans. 2* **77**, 1891 (1981).

<sup>14</sup>R. G. Palmer, D. L. Stein, E. Abrahams, and P. W. Anderson, *Phys. Rev. Lett.* **53**, 958 (1984).

<sup>15</sup>G. H. Fredrickson and H. C. Anderson, *Phys. Rev. Lett.* **53**, 1244 (1984).

<sup>16</sup>T. G. Fox and P. J. Flory, *J. Am. Chem. Soc.* **70**, 2384 (1948); *J. Appl. Phys.* **21**, 581 (1950).

<sup>17</sup>See, e.g., (a) R. N. Haward, *The Physics of Glassy Polymers* (Wiley, New York, 1973); (b) M. H. Cohen and G. S. Grest, *Phys. Rev. B* **20**, 1077 (1979), and references therein.

<sup>18</sup>R. D. Batie, J. L. Viovy, and L. Monnerie, *J. Chem. Phys.* **81**, 567 (1984).

<sup>19</sup>See, e.g., Ref. 17(a) Introduction.

<sup>20</sup>A. Kolinski, J. Skolnick, and R. Yaris (work in progress).

<sup>21</sup>J. Klein and B. J. Briscoe, *Proc. R. Soc. London Ser. A* **365**, 53 (1979).

<sup>22</sup>S. D. Druger, A. Nitzan, and M. A. Ratner, *J. Chem. Phys.* **79**, 3113 (1983).